

# Crystallization kinetics of metallic glasses

## Transformation diagrams

Joan Josep Suñol · J. Bonastre

NATAS2009 Special Issue  
© Akadémiai Kiadó, Budapest, Hungary 2010

**Abstract** In this study, the temperature-heating rate diagram of the main crystallization process of two metallic glasses,  $\text{Fe}_{74}\text{Ni}_{3.5}\text{Mo}_3\text{B}_{16}\text{Si}_{3.5}$  and  $\text{Fe}_{41}\text{Ni}_{38}\text{Mo}_3\text{B}_{18}$ , was obtained from one experimental differential scanning calorimetry (DSC) scan and the knowledge of their activation energy as determined by an isoconversional method. A good concordance was observed between the diagram curves obtained by calculation (isoconversional approach) and the experimental data, which verifies the reliability of the method and the validity of the kinetic approach in these alloys.

**Keywords** Transformation diagrams · Kinetics · Metallic glasses

## Introduction

The knowledge of the crystallization kinetics of materials is important to control their structure and properties. Several authors deal with calculating the amount of transformed material during crystallization. They have led to the determination of temperature–time–transformation, T-T-T, curves for the description of the isothermal crystallization reaction since the study of Uhlmann [1]. Other transformation diagrams have been introduced [2] to describe non-equilibrium crystallization under continuous heating or cooling regimes, namely the T-HR-T (temperature–heating rate–transformation) and T-CR-T (temperature–cooling rate–transformation) diagrams.

It is known that nanostructured materials developed by controlled crystallization yield extremely good properties, offering a field for many technological applications [3, 4]. Several techniques have been utilized to investigate the kinetics of crystallization processes. The recent literature demonstrates that this field presents a great scientific interest [5, 6]. In particular, the thermoanalytical techniques (TA), such as differential thermal analysis (DTA), thermogravimetry (TG) and differential scanning calorimetry (DSC) are ones of the most often applied to assess crystallization kinetics. From DSC data, several models have been developed to analyze experimental data under isothermal or continuous rate conditions. In this study, we analyze the crystallization process of two Fe-rich metallic glasses by applying an isoconversional method. Once activation energy has been determined, one can construct the transformation diagrams [7]. In order to develop nanocrystalline structure, transformation diagrams permit us the selection of annealing treatments to produce materials with the desired nanostructure.

## Experimental

In this study, both Fe-rich alloys were obtained by rapid solidification, i.e., melt spinning. The nominal composition of the metallic glass ribbons studied were:  $\text{Fe}_{74}\text{Ni}_{3.5}\text{Mo}_3\text{B}_{16}\text{Si}_{3.5}$  and  $\text{Fe}_{41}\text{Ni}_{38}\text{Mo}_3\text{B}_{18}$ , labeled as alloys A and B, respectively. The amorphous (as confirmed by X-ray analysis) ribbons were produced by quenching the molten alloy on the surface of a rapidly spinning (about  $35 \text{ m s}^{-1}$ ) Cu wheel. The working atmosphere was inert, Ar.

Differential scanning calorimetry was done with an argon purging gas. These measurements were necessary for the study of the crystallization behavior of the melt-spun

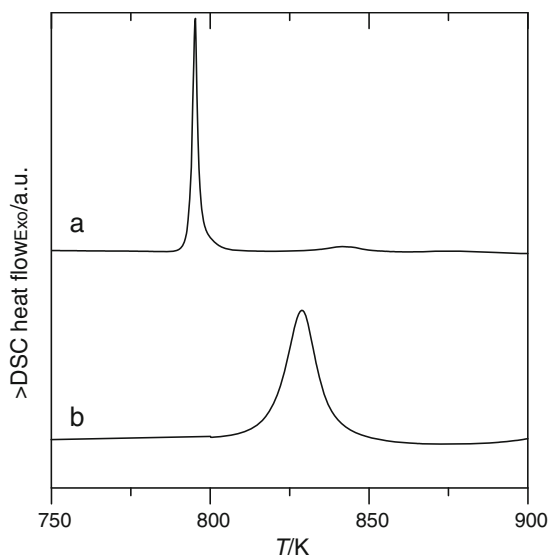
J. J. Suñol (✉) · J. Bonastre  
GRMT, Campus Montilivi s/n, University of Girona,  
17071 Girona, Spain  
e-mail: joanjosep.sunyol@udg.edu

ribbons in the case of an amorphous phase. Thermal stability was analyzed via non-isothermal experiments. The scanning rates,  $\beta$ , employed varied from 5 to 80 K min<sup>-1</sup>.

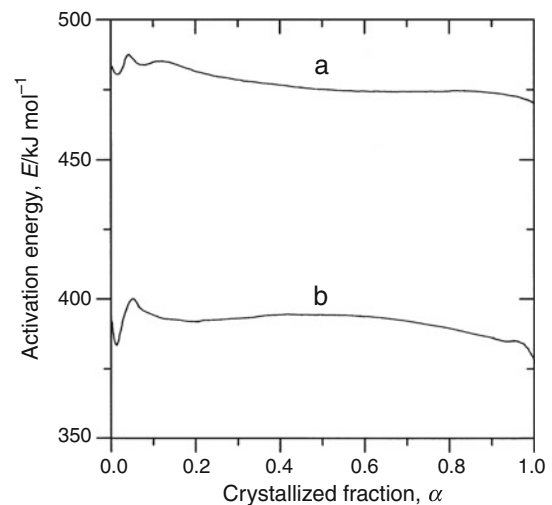
## Results

Figure 1 shows the DSC scans corresponding to alloys A and B heated at 10 K min<sup>-1</sup>. Alloy A has a wider temperature range whereas in alloy A peak is narrower. The crystallization process of alloy A begins at lower temperature ( $\sim 790$  K) than the corresponding temperature of alloy B ( $\sim 815$  K).

The apparent activation energies,  $E$ , can be obtained with several linear methods as the Kissinger [8] or the Ozawa [9] methods. The calculated Kissinger values are  $478 \pm 7$  and  $382 \pm 5$  kJ mol<sup>-1</sup> for alloys A and B, respectively. Nevertheless, as well known these methods use logarithm linearization and not consider all data from DSC measurements, only peak temperature at each heating rate. For that reason they are very sensitive to the experimental errors. Furthermore, to study initial stages of crystallization involves transformed fractions lower than 0.2. Thus, models based on peak temperature induce error because transformed fraction at peak temperature is usually  $\sim 0.5$ . Several more complex methods based on isoconversional transformed fraction can be applied to obtain the activation energy. A revision of the isoconversional methods is given in [10]. Obviously, the results are influenced by the activation energy selected in the calculation. If an isoconversional approach is used, it is possible to obtain the dependence with the transformed fraction.



**Fig. 1** DSC scans of alloys (a) Fe<sub>74</sub>Ni<sub>3.5</sub>Mo<sub>3</sub>B<sub>16</sub>Si<sub>3.5</sub> and (b) Fe<sub>41</sub>Ni<sub>38</sub>Mo<sub>3</sub>B<sub>18</sub> at a heating rate of 10 K min<sup>-1</sup>



**Fig. 2** Activation energy as a function of the transformed fraction for alloys (a) Fe<sub>74</sub>Ni<sub>3.5</sub>Mo<sub>3</sub>B<sub>16</sub>Si<sub>3.5</sub> and (b) Fe<sub>41</sub>Ni<sub>38</sub>Mo<sub>3</sub>B<sub>1</sub>

## Transformation diagrams

The production of a controlled nanostructure from the amorphous state has become of special interest for technological applications. It can be also interesting to obtain it with only few data and without the knowledge of the crystallization governing mechanism. If crystallization proceeds via simultaneous nucleation and interface controlled growth with time-independent rates in both nucleation,  $I$ , and crystal growth,  $u$ , classical theory gives the crystallized transformed fraction,  $\alpha$ , under isothermal regime at temperature,  $T$ , and annealing time,  $t$ , as

$$\alpha(T, t) = 1 - \exp \left[ -A_m \int_0^t I(\tau) [u(T)]^m (t - \tau)^m d\tau \right] \quad (1)$$

where it is assumed that nucleation takes place at a time,  $\tau$ , through regions of the material which have not been already transformed,  $m = 1, 2, 3$  is the number of dimensions of the nuclei which grow at the same rate, and  $A_m$  are suitable geometrical constants.

Similarly, when crystallization proceeds from preexisting nuclei by interface controlled growth and no nuclei are formed during the transformation the corresponding equations giving the crystallized fraction may be written as

$$\alpha(T, t) = 1 - \exp \left[ -B_m \int_0^t [u(T)]^m (t - \tau)^{m-1} d\tau \right] \quad (2)$$

where  $B_m$  is a constant which includes geometrical factors and density of preexisting nuclei. Both equations are possible particular examples of models associated to specific crystallization mechanism. Nevertheless, it can be

interesting to obtain information directly from continuous heating experiments to build the T-HR-T diagrams.

Continuous heating

To avoid a significant crystalline fraction during initial cooling, quick enough cooling rate,  $c$ , is necessary on cooling to the glass transition. The crystallization temperature on subsequent reheating may depend to some extent on cooling rate due to the fact that, at any time and temperature an embryo (formed initially on cooling the liquid) may become supercritical when reheating. Assuming that the glass is formed with crystalline fractions less than  $10^{-9}$  at the glass transition, the crystalline fraction obtained after continuous heating to temperature,  $T$ , at a constant heating rate,  $\beta$ , may be written, for  $m$ -dimensional interface controlled growth, as

$$\alpha(T, \beta) = 1 - \exp \left[ -A_m \int_{T_m}^{T'} I(T) dT \left[ \int_T^{T'} [u(T'') dT'']^m \right] \beta^{-(m+1)} \right] \tag{3}$$

for homogeneous nucleation and no pre-existing nuclei, or

$$\alpha(T, \beta) = 1 - \exp \left[ -B_m \left[ \int_{T_m}^{T'} [u(T) dT]^m \right] \beta^{-m} \right] \tag{4}$$

for growth of pre-existing nuclei.

The approximate treatment of crystallization on heating at a constant rate,  $\beta$ , may be written in integral form as

$$\alpha(T, \beta) = 1 - \exp \left[ - \left[ \int_{T_m}^{T'} [K(T) dT]^n \right] \beta^{-n} \right] \tag{5}$$

where the rate constant  $K(T)$  can be written in the Arrhenius form.

$$K(T) = k_0 \exp(-E/RT) \tag{6}$$

Once the value of the apparent activation energy is known, it is usual to evaluate a function  $f(\alpha)$  describing the crystallization from the continuous heating experiments and to compare the results to value obtained in other experiments, i.e., isothermal [11]. Nevertheless, in several cases complex or overlapping crystallization processes occur simultaneously and a kinetic model governing crystallization cannot be deduced correctly. However, a method of obtaining transformation diagrams from non-isothermal data can be applied. In this study,  $E$  values are obtained (see Fig. 2) by the model-free developed by Vyazovkin [12]. T-HR-T curves can be calculated [7] by

integration of the reaction rate equation [13] under continuous heating rate

$$\beta = \frac{k_0 RT^2 \exp(-E/RT)}{E \int_0^\alpha \frac{d\alpha}{f(\alpha)}} \tag{7}$$

By using the following equation, one can solve the integral of previous equation even if the value of  $f(\alpha)$  is unknown:

$$\int_0^\alpha \frac{d\alpha}{k_0 f(\alpha)} = \int_0^T \frac{\exp(-E/RT)}{\beta} dT \tag{8}$$

To calculate T-HR-T diagrams, it is necessary to solve numerically the right integral of Eq. 7. For the integral isoconversional methods, assumption of a constant value of the activation energy is necessary and implicit for the separation of variables in Eq. 8 and for the derivation of this equation [14]. For it, an average  $E$  value of the central zone  $\langle 0.2, 0.8 \rangle$  of the transformed fraction was used. Only to build the 0.1-transformed fraction curve the activation energy was the average value in the zone  $\langle 0.07, 0.13 \rangle$ . Thus, the only experimental data are one calorimetric curve ( $\beta = 10 \text{ K min}^{-1}$ ) and the activation energy of the process. In the central zone, the values are nearly constant:  $\sim 475$  and  $\sim 390 \text{ kJ mol}^{-1}$  for alloys A and B, respectively.

This approach is applied to the study of the crystallization behavior of both amorphous alloys obtained using the melt-spinning technique. Figures 3 (alloy A) and 4 (alloy B) show the T-HR-T curves calculated with the experimental data that correspond to  $\alpha$  values of 0.1, 0.5, and 0.9. Curves were compared with the experimental data

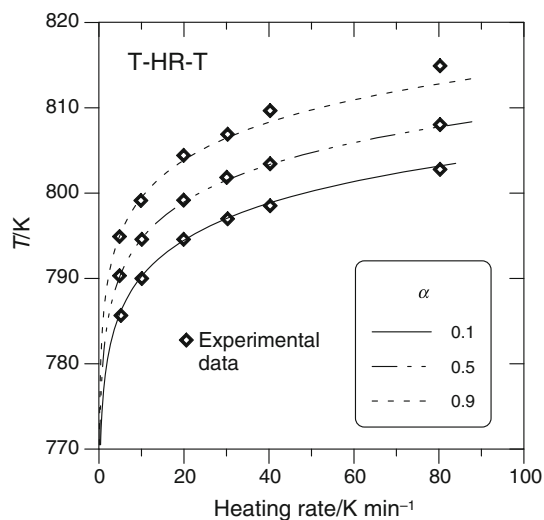


**Fig. 3** T-HR-T curves that correspond to main crystallization process of  $\text{Fe}_{74}\text{Ni}_{3.5}\text{Mo}_3\text{B}_{16}\text{Si}_{3.5}$  metallic glass. Experimental data (symbols) and isoconversional calculated curves (lines) for transformed fractions (0.1, 0.5, and 0.9)

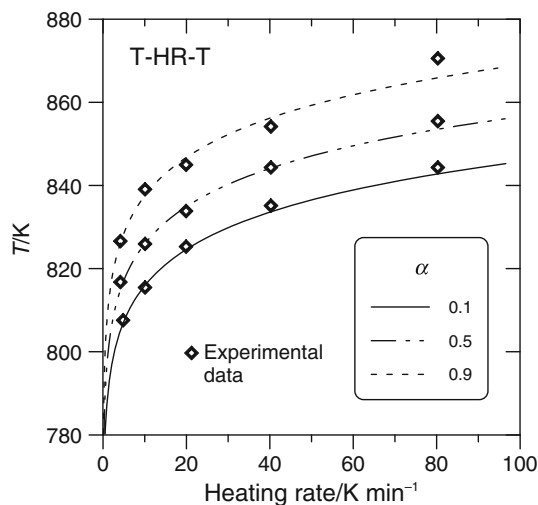


**Fig. 4** T-HR-T curves that correspond to main crystallization process of  $\text{Fe}_{41}\text{Ni}_{38}\text{Mo}_3\text{B}_{18}$  metallic glass. Experimental data (*symbols*) and isoconversional calculated curves (*lines*) for transformed fractions (0.1, 0.5, and 0.9)

from measurements at other heating rates to check the methodological validity. A good concordance was observed between the diagram curves obtained by calculation (isoconversional approach) and the experimental data, which verifies the reliability of the method and the validity of the rate constant model description. The poor approach was found at the higher heating rate ( $80 \text{ K min}^{-1}$ ). The major application of the T-HR-T curves should be for prediction of the amount of material crystallized during treatment of the samples at a certain constant heating rate. Thus, sometimes it is more important the accuracy of the prediction than the accuracy of the kinetic analysis.

## Conclusions

The temperature–heating rate–transformation diagrams of the main crystallization process of two metallic glasses were built. All the transformation curves are obtained from non-isothermal data. A good concordance was observed

between the T-HR-T diagram curves obtained by calculation and the experimental data, which verifies the reliability of the approach and the capacity of prediction.

**Acknowledgements** Financial support from DURSI [2009SGR374] is acknowledged.

## References

1. Uhlmann DR. A kinetic treatment of glass formation. *J Non-Cryst Solids*. 1972;7:337–48.
2. Suriñach S, Baró MD, Diego JA, Clavaguera N, Clavaguera-Mora MT. A new temperature versus heating rate transformation (T-HR-T) diagram—application to study the crystallization behavior of  $\text{Fe}_{67.5}\text{Co}_{15}\text{Nb}_{1.5}\text{B}_{16}$ . *Acta Metall Mater*. 1992;40:37–42.
3. Clavaguera-Mora MT, Clavaguera N, Crespo D, Pradell T. Crystallization kinetics and microstructure development in metallic systems. *Prog Mater Sci*. 2002;47:559–619.
4. McHenry ME, Willard MA, Laughlin DE. Amorphous and nanocrystalline materials for applications as soft magnets. *Prog Mater Sci*. 1999;44:291–433.
5. Criado JM, Sánchez-Jiménez PE, Pérez-Maqueda LA. Critical study of the isoconversional methods of kinetic analysis. *J Therm Anal Calorim*. 2008;92:199–203.
6. González A, Bonastre J, Escoda L, Suñol JJ. Thermal analysis of Fe(Co, Ni) based alloys prepared by mechanical alloying. *J Therm Anal Calorim*. 2007;87:255–8.
7. Suñol JJ, Berlanga R, Clavaguera-Mora MT, Clavaguera N. Modelling crystallization process: transformation diagrams. *Acta Mater*. 2002;50:4783–90.
8. Kissinger HE. Reaction kinetics in differential thermal analysis. *Anal Chem*. 1957;29:1702–6.
9. Ozawa T. A new method of analyzing thermogravimetric data. *Bull Chem Soc Jpn*. 1965;38:1881–6.
10. Málek J. Kinetic analysis of crystallization processes in amorphous materials. *Thermochim Acta*. 2002;355:239–53.
11. Bonastre J, Chognon E, Escoda L, Güell JM, Hernando B, Suñol JJ. Development of nanostructured materials by mechanical alloying and/or rapid solidification. *Phys Stat Solid (c)*. 2009;6:2156–9.
12. Vyazovkin S. Advanced isoconversional method. *J Therm Anal*. 1997;49:1493–9.
13. Suñol JJ, Clavaguera N, Mora MT. Thermal stability study of Fe–Ni based alloys: determination of T-HR-T and T-T-T diagrams. *J Therm Anal*. 1998;52:853–62.
14. Simon P. Isoconversional methods. Fundamentals, meaning and applications. *J Therm Anal Calorim*. 2004;76:123–32.